Electronic Supplementary Material (ESI) for Journal of Materials Chemistry C.

Supporting Information:

Intrinsic vs. extrinsic STE emission enhancement in *ns*^{2} ion doped metal (Cd, In) halide hybrids

Deep Kumar Das,[a] Rangarajan Bakthavatsalam,[a] Venkatesha R Hathwar,[b] Raghavaiah Pallepogu,[c] Janardan Kundu[a]*

[a] Indian Institute of Science Education and Research (IISER) Tirupati, Tirupati, Andhra Pradesh 517507, India; orcid.org/0000-0003-4879-0235; Email: janardan@iisertirupati.ac.in

[b] School of Physical and Applied Sciences, Goa University, Goa 403206, India

[c] Department of Chemistry, Central University of Karnataka, Kalaburagi, Karnataka 585367, India

Materials and Methods

Materials: Cadmium(II) chloride hemi(pentahydrate), Indium (III) oxide (99%), Antimony (III) oxide (99%), Antimony (III) chloride (99%), Bismuth (III) chloride (98%), 1-(2-aminoethyl)piperazine (99%), Hydrochloric acid (37%) and Acetone were purchased from Sigma Aldrich. All chemicals were used without further purification.

Synthesis of AEPipInCl

Single crystals of AEPipInCl were prepared by dissolving 0.5 mmol of In_2O_3 (138.815 mg) and 2 mmol of 1-(2-aminoethyl)piperazine (262 μL) in 10 mL HCl at 90 °C. The resultant clear solution was further heated at the same temperature for 2 hours and cooled to room temperature naturally to obtain colourless crystals.

Yield: 0.550 g (82%)

Synthesis of AEPipInSbCl:

Single crystals of AEPipInSbCl were synthesized by dissolving 0.475 mmol of In_2O_3 (131.874 mg) and 0.025 mmol of Sb_2O_3 (7.288 mg) in 4 mL HCl through sonication at room temperature. After getting a clear solution, 2 mmol of 1-(2-aminoethyl)piperazine (262 μL) was added to the clear precursor solution in the ice bath with continuous stirring. The mixture was heated in an oil bath at 90 °C till complete dissolution with further addition of HCl. The clear solution was heated for 2 hours, and it was allowed to cool naturally. Colourless crystals which emit yellow color under UV light were obtained. The crystals were filtered, washed with acetone, and dried in vacuum at 55 °C overnight. For doping various amounts of Sb, the reaction was done in the same manner by replacing In_2O_3 partially with different concentrations of Sb_2O_3

[0.005 (1.4576 mg), 0.0125 (3.644 mg), 0.025 (7.288 mg), 0.05 (14.576 mg), 0.165 (48.1008 mg), 0.25 (72.88 mg) mmol]

Yield: 0.650 g (77%)

Synthesis of AEPipInBiCl:

Single crystals of AEPipInBiCl were prepared in the similar way like AEPipInSbCl, but $BiCl_3$ was used instead of Sb_2O_3. Here, 0.45 mmol of In_2O_3 (124.934 mg) and 0.1 mmol of $BiCl_3$ (31.534 mg) were dissolved in 4 mL HCl through sonication at room temperature. After getting a clear solution, 2 mmol of 1-(2-aminoethyl)piperazine (262 µL) was added to the clear precursor solution in the ice bath with continuous stirring. The mixture was heated in an oil bath at 90 °C till complete dissolution with further addition of HCl. The clear solution was heated for 2 hours, and it was allowed to cool naturally to obtain colourless crystal.

Yield: 0.396 g (75%)

Synthesis of AEPipCdCl

Single crystals of **AEPipCdCl** were prepared by dissolving 1 mmol of $CdCl_2$ (228.36 mg) and 2 mmol of 1-(2-aminoethyl)piperazine (262 µL) in 10 mL HCl at 90 °C. The resultant clear solution was further heated at the same temperature for 2 hours and cooled to room temperature naturally to obtain colourless crystals.

Yield: 0.490 g (85%)

Synthesis of AEPipCdSbCl:

Single crystals of AEPipCdSbCl were synthesized similarly. 0.95 mmol of $CdCl_2$ (216.942 mg) and 0.025 mmol of Sb_2O_3 (7.288 mg) were dissolved in 3 mL HCl through sonication at room temperature. After getting a clear solution, 2 mmol of 1-(2-aminoethyl)piperazine (262 µL) was added to the clear precursor solution in the ice bath with continuous stirring with further addition of HCl. The mixture was heated in an oil bath at 90 °C till complete dissolution. The heating was turned off once a clear solution was obtained, and it was allowed to cool naturally. Colorless crystals which emit yellow under UV light were obtained within a few hours. The crystals were filtered, washed with acetone, and dried in vacuum at 55 °C overnight. For doping various amounts of Sb, the reaction was done in the same manner by replacing $CdCl_2$ partially with different concentrations of Sb_2O_3 [0.005 (1.4576 mg), 0.0125 (3.644 mg), 0.025 (7.288 mg), 0.05 (14.576 mg), 0.165 (48.1008 mg), 0.25 (72.88 mg) mmol].

Yield: 0.396 g (75%)

Synthesis of AEPipSbCl:

Powders of AEPipSbCl were prepared by dissolving 1 mmol of $SbCl_3$ (228.13 mg) in 4 mL HCl through sonication at room temperature. After getting a clear solution, 2 mmol of 1-(2-aminoethyl)piperazine (262 µL) was added to the clear precursor solution in an ice bath with continuous stirring. Then 10 mL acetone was added to the mixture in the precursor solution with vigorous stirring at room temperature. The resulting powder emits yellow under UV light (365 nm) excitation. The powder was filtered, washed with acetone, and dried in a vacuum oven at 55 °C overnight.

Synthesis of AEPipBiCl:

Powders of AEPipBiCl were synthesized by dissolving 1 mmol of $BiCl_3$ (315.34 mg) in 4 mL HCl through sonication at room temperature. After getting a clear solution, 2 mmol of 1-(2-aminoethyl)piperazine (262 µL) was added to the clear precursor solution in an ice bath with continuous stirring. Then 10 mL acetone was added to the mixture in the precursor solution with vigorous stirring at room temperature. The powder was filtered, washed with acetone, and dried in a vacuum oven at 55 °C overnight.

Characterization methods:

Solid-state UV vis absorption measurements were performed in an Agilent Cary Series UV-Vis-NIR Spectrophotometer with an integrating sphere accessory. Steady-state PL, PLE, lifetime, low-temperature PL, PLE, and absolute quantum yield of crystals were measured in an Edinburgh FLS1000 photoluminescence spectrometer, attached with Optistat DN cryostat. The temperature was controlled using a Mercury iTC temperature controller (Oxford instruments). The sample was excited using a xenon lamp, and emission was collected from 320 nm to 800 nm. Powder X-ray diffraction of samples was recorded on Rigaku SmartLab with a Cu $K\alpha1$ source (λ = 1.5406 Å). Single-crystal X-ray diffraction data were collected on a Bruker APEX II single-crystal X-ray CCD diffractometer having graphite monochromatized (Mo Kα, λ = 0.71073 Å) radiation at 100.0 K. Data reduction was performed using APEX II software. Intensities for absorption were corrected with SADABS, and using Olex2, the structure was solved with the SHELXS structure solution program using direct methods and refined with the SHELXL refinement package using least-squares minimization, with anisotropic displacement parameters for all non-H atoms. In all crystal structures, hydrogen atoms were located through the Fourier difference electron density maps. Technical details of data acquisition, selected crystal refinement results, and selected bond distances and angles are reported in Tables S5−S43. Mercury software was used to prepare *ORTEP* and packing diagrams. CIF files are available at www.ccdc.cam.ac.uk/data (CCDC nos. 2209713, 2209716, 2209720, 2209724). Samples for powder X-ray diffraction were prepared by mechanical grinding of single crystals. Scanning Electron Microscopy (SEM) imaging and mapping were performed by Zeiss™ Ultra Plus field-emission scanning electron microscope. X-ray photoelectron spectroscopy (XPS) characterization was performed with ESCALab spectrometer having Al Kα X-ray source (*hυ*=1486.6 eV) operating at 150 W using a Physical Electronics 04-548 dual Mg/Al anode and in a UHV system with a base pressure of $\leq 5 \times 10^{-9}$ Torr. TGA measurements were performed using a TAG system (Mettler-Toledo, Model TGA/SDTA851e), and samples were heated in the range of room temperature to 800°C at a heating rate of 10°C/min under nitrogen atmosphere.

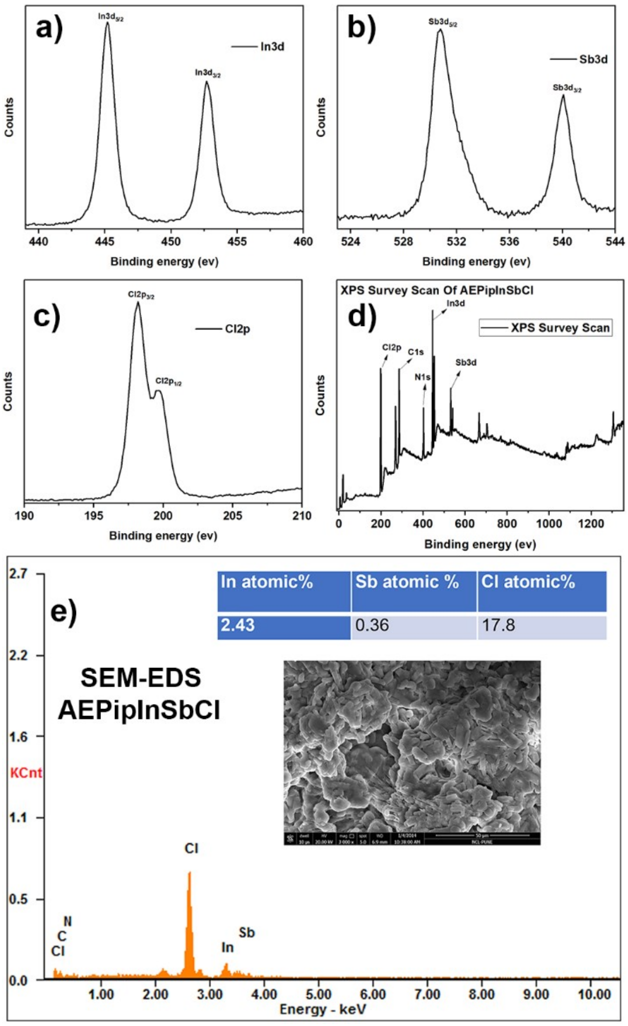

In atomic%	Sb atomic %	Cl atomic%
2.43	0.36	17.8

Figure S1: (a-d) XPS spectra and e) EDS spectra of AEPipInSbCl showing presence of In and Sb. Inset shows the image of crystal under an SEM. Inset table depicting Atomic percentages of In and Sb measured from the EDS.

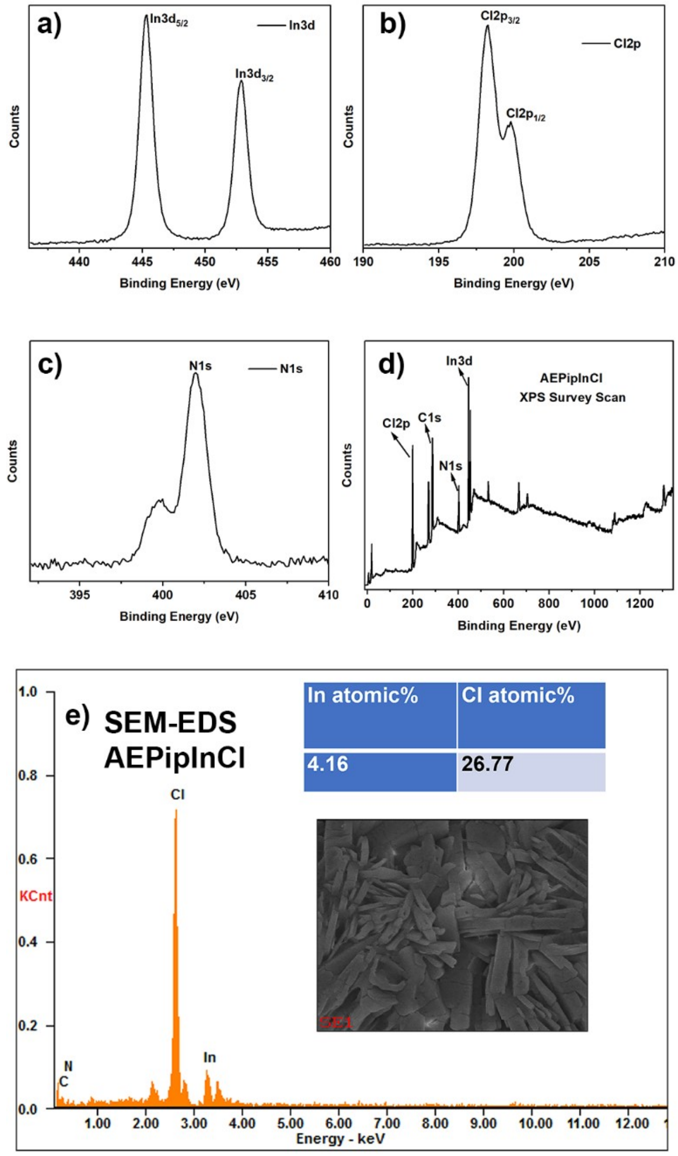

In atomic%	Cl atomic%
4.16	26.77

Figure S2: (a-d) XPS spectra and e) EDS spectra of AEPipInCl showing presence of In and Cl. Inset shows the image of crystal under an SEM. Inset table depicting Atomic percentages of In and Cl measured from the EDS.

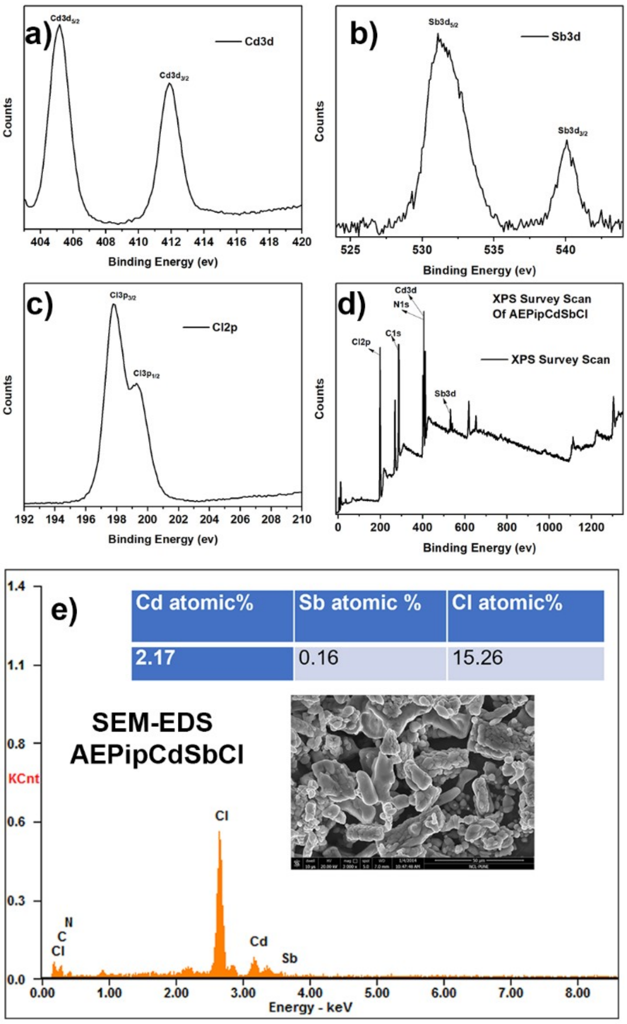

Cd atomic%	Sb atomic %	Cl atomic%
2.17	0.16	15.26

Figure S3: (a-d) XPS spectra and e) EDS spectra AEPipCdSbCl showing presence of Cd and Sb. Inset shows the image of crystal under an SEM. Inset table depicting Atomic percentages of Cd and Sb measured from the EDS.

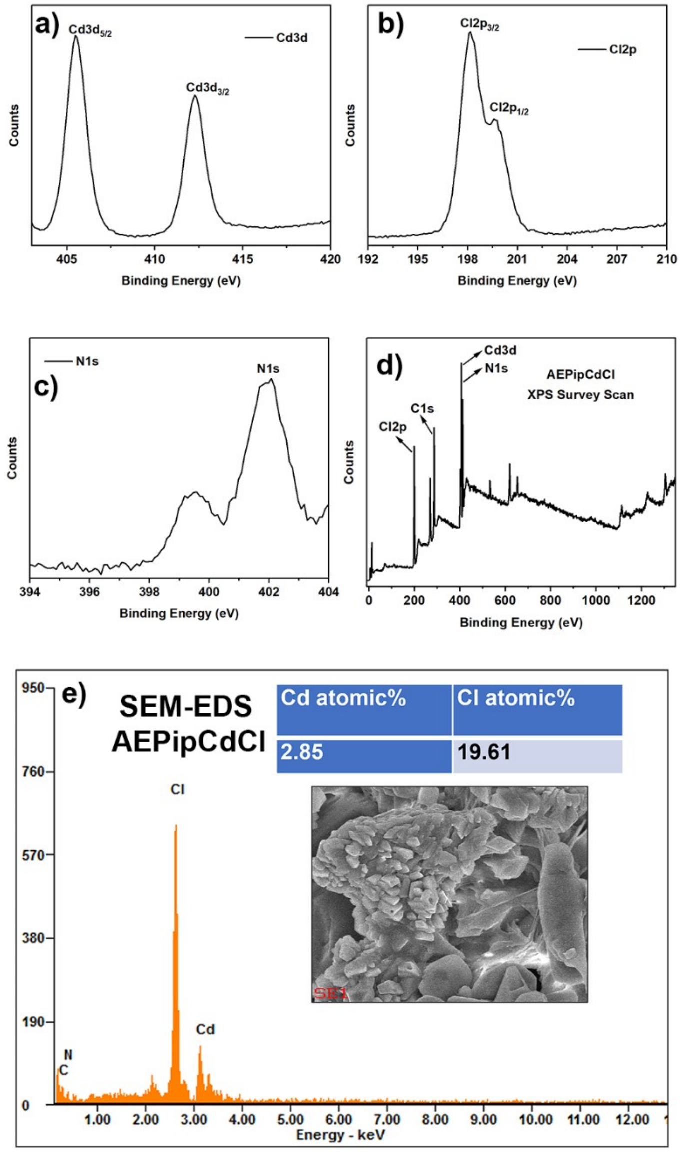

Cd atomic%	Cl atomic%
2.85	19.61

Figure S4: (a-d) XPS spectra and e) EDS spectra AEPipCdCl showing presence of Cd and Cl. Inset shows the image of crystal under an SEM. Inset table depicting Atomic percentages of Cd and Cl measured from the EDS.

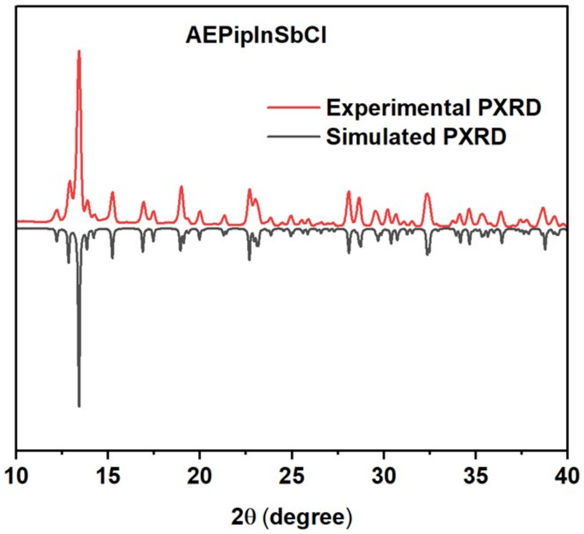

Figure S5: Comparison of simulated and experimental PXRD of AEPipInSbCl system.

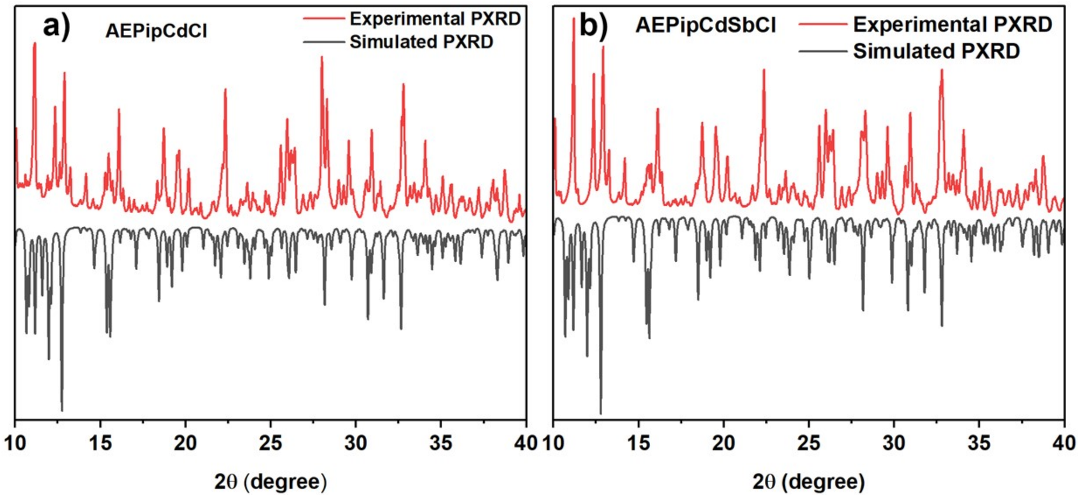

Figure S6: Comparison of simulated and experimental PXRD of a) AEPipCdCl and b) AEPipCdSbCl system.

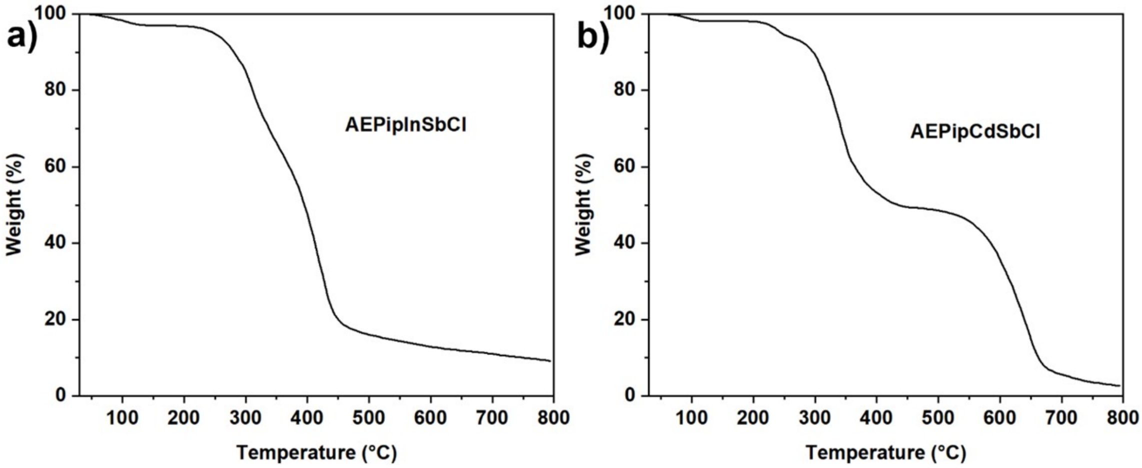

Figure S7: Thermogravimetric analysis (TGA) of a) AEPipInSbCl; b) AEPipCdSbCl system.

Table S1: Dopant ‘Sb’ concentrations derived from ICP measurements for different feed concentration of ‘Sb’ in AEPipInSbCl and AEPipCdSbCl system.

AEPipInSbCl	
Feed Concentration of Sb(%)	Sb Concentration (from ICP experiment)(%)
2.5	0.82
10	3.26
50	30.35

AEPipCdSbCl	
Feed Concentration of Sb(%)	Sb Concentration (from ICP experiment)(%)
2.5	0.28
10	1.39
50	6.10

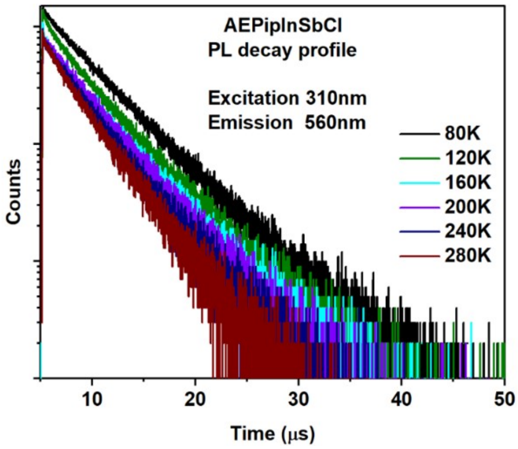

Figure S8: PL decay curve of AEPipInSbCl: Sb 5% at different temperatures.

Table S2: PL lifetime values of AEPipInSbCl: Sb 5% at different temperatures.

AEPipInSbCl					
Temperature (K)	τ_1 (μs)	Rel%	τ_2 (μs)	Rel%	$\tau_{average}$ (μs)
80K	4.79 μs	97.53%	1.35 μs	2.47%	4.7 μs
120K	4.30 μs	93.47%	1.03 μs	6.53%	4.1 μs
160K	4.2 μs	97.05%	0.73 μs	2.95%	4.1 μs
200K	3.95 μs	100%			3.95 μs
240K	3.6 μs	97.60%	1.1 μs	2.40%	3.6 μs
280K	3.4 μs	95.16%	0.96 μs	4.84%	3.3 μs

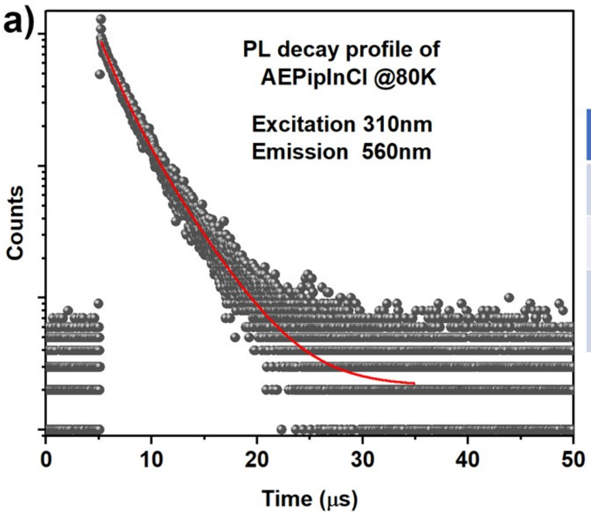

AEPipInCl		
τ_1	3.58 μs	66.34%
τ_2	1.64 μs	33.66%
$\tau_{average}$ = 2.9 μs		

Figure S9: PL decay curve and corresponding lifetime value of host AEPipInCl collected for 560 nm emission by exciting at 310 nm at 80 K.

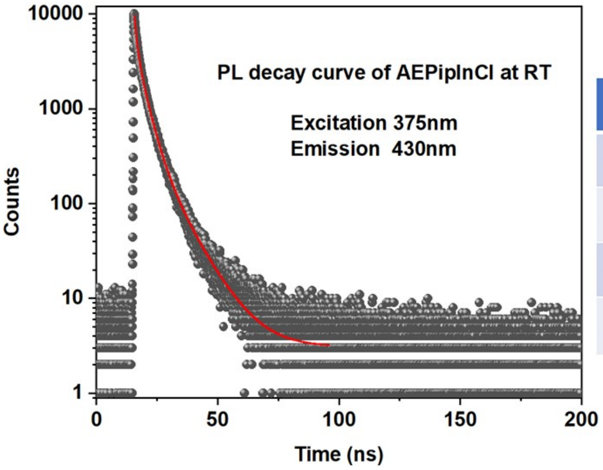

AEPipInCl		
τ_1	3.4 ns	66.34%
τ_2	9.39 ns	33.66%
τ_3	0.87 ns	17.17%
$\tau_{average}$ = 4.4 ns		

Figure S10: PL decay curve and corresponding lifetime value of host AEPipInCl collected for 430 nm emission by exciting at 375 nm.

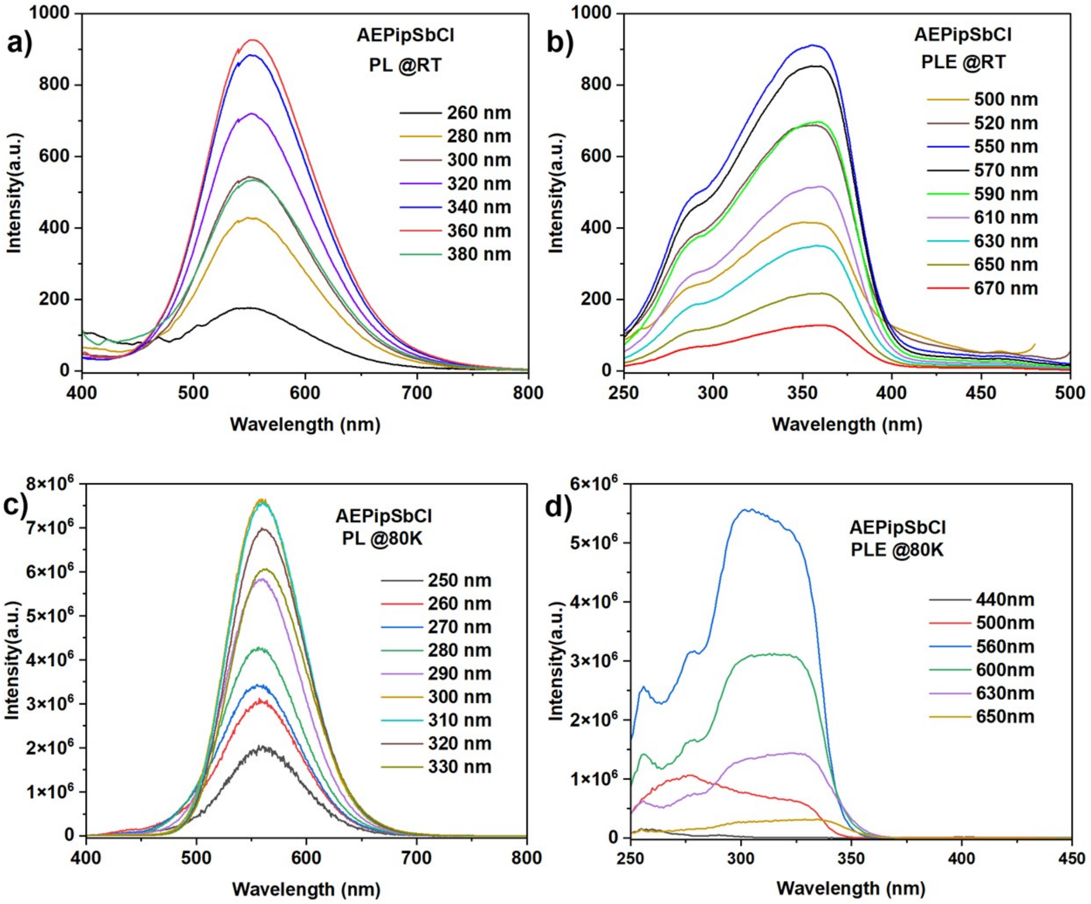

Figure S11: a) PL and b) PLE of AEPipSbCl collected at different excitation and emission wavelength at room temperature; c) PL and d) PLE of AEPipSbCl collected at different excitation and emission wavelength at 80 K.

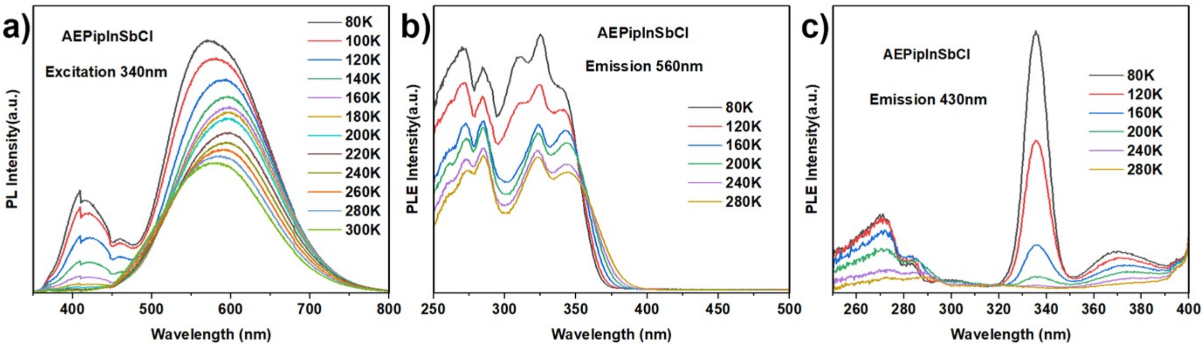

Figure S12: Temperature-dependent a) PL collected at 340 nm excitation; PLE collected at b) 560 nm emission and c) 430 nm emission of AEPipInSbCl: Sb 5% susyem.

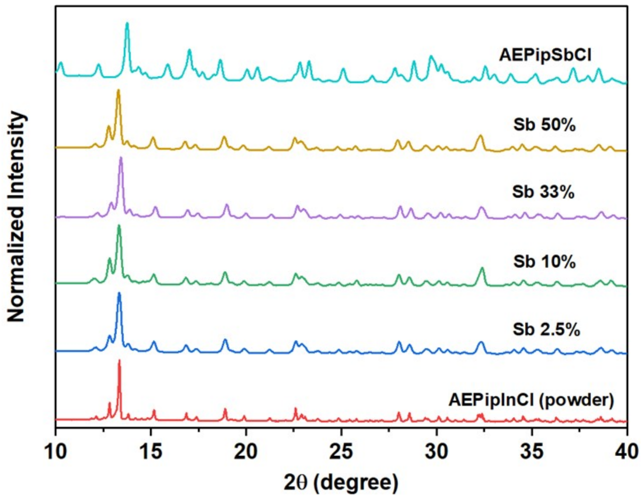

Figure S13: PXRD pattern of AEPipInCl with different feed concentration (%) of Sb.

Table S3: PL lifetimes of AEPipInSbCl with different feed concentrations of dopant 'Sb' collected at 560 nm emission by exciting at 310 nm.

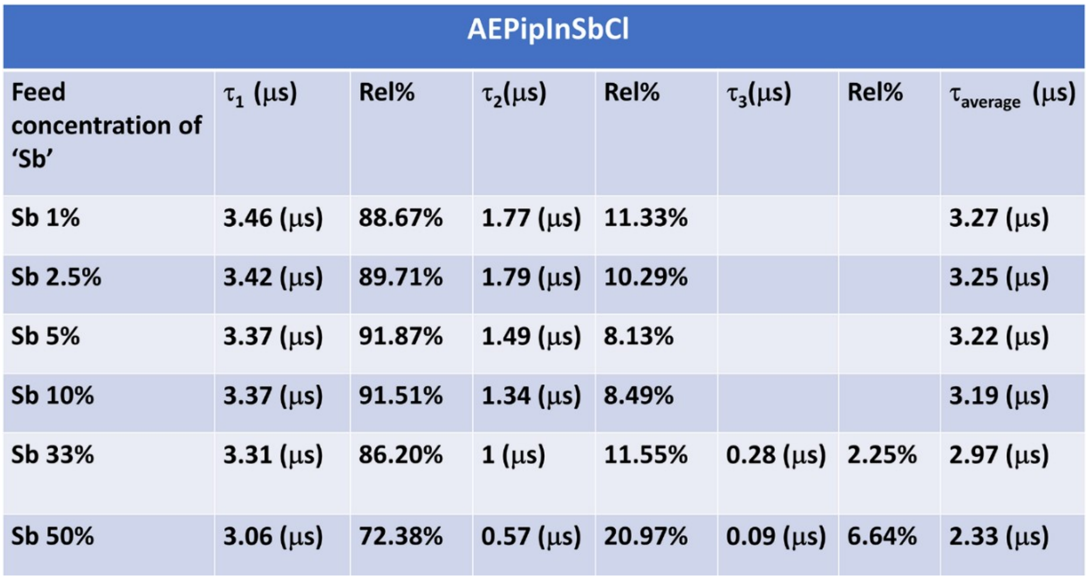

AEPipInSbCl							
Feed concentration of 'Sb'	τ_1 (μs)	Rel%	τ_2(μs)	Rel%	τ_3(μs)	Rel%	$\tau_{average}$ (μs)
Sb 1%	3.46 (μs)	88.67%	1.77 (μs)	11.33%			3.27 (μs)
Sb 2.5%	3.42 (μs)	89.71%	1.79 (μs)	10.29%			3.25 (μs)
Sb 5%	3.37 (μs)	91.87%	1.49 (μs)	8.13%			3.22 (μs)
Sb 10%	3.37 (μs)	91.51%	1.34 (μs)	8.49%			3.19 (μs)
Sb 33%	3.31 (μs)	86.20%	1 (μs)	11.55%	0.28 (μs)	2.25%	2.97 (μs)
Sb 50%	3.06 (μs)	72.38%	0.57 (μs)	20.97%	0.09 (μs)	6.64%	2.33 (μs)

Table S4: PLQY values of a) AEPipInSbCl and b) AEPipCdSbCl system for different feed concentration of Sb.

a)

AEPipInSbCl	
Feed concentration of 'Sb' (%)	**PLQY (%)**
1	72.4
2.5	74.44
5	69.29
10	61.89
33	23.13
50	7.95

b)

AEPipCdSbCl	
Feed concentration of 'Sb' (%)	**PLQY (%)**
1	92.21
2.5	91.18
5	98.59
10	98.33
33	83.25
50	73.15

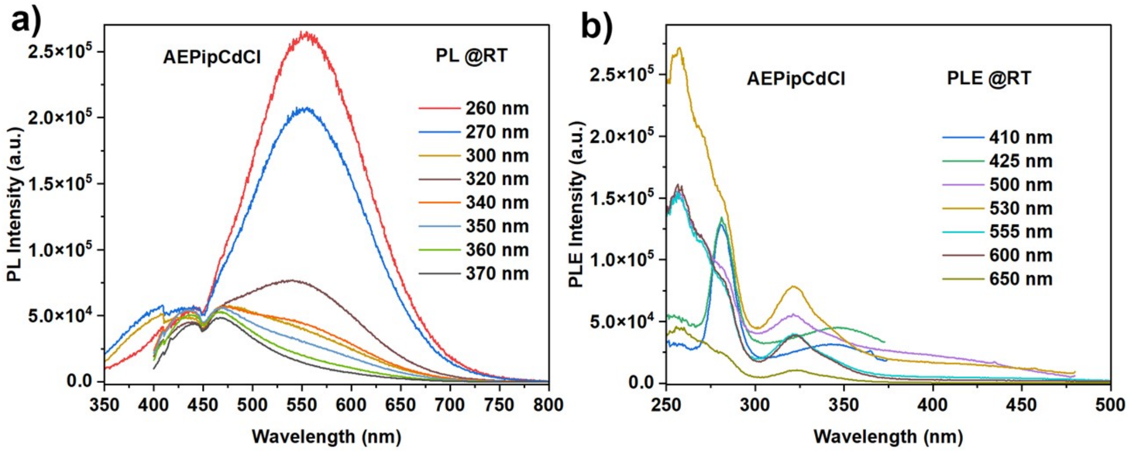

Figure S14: Room temperature a) PL and b) PLE of AEPipCdCl collected at different excitation and emission wavelengths respectively.

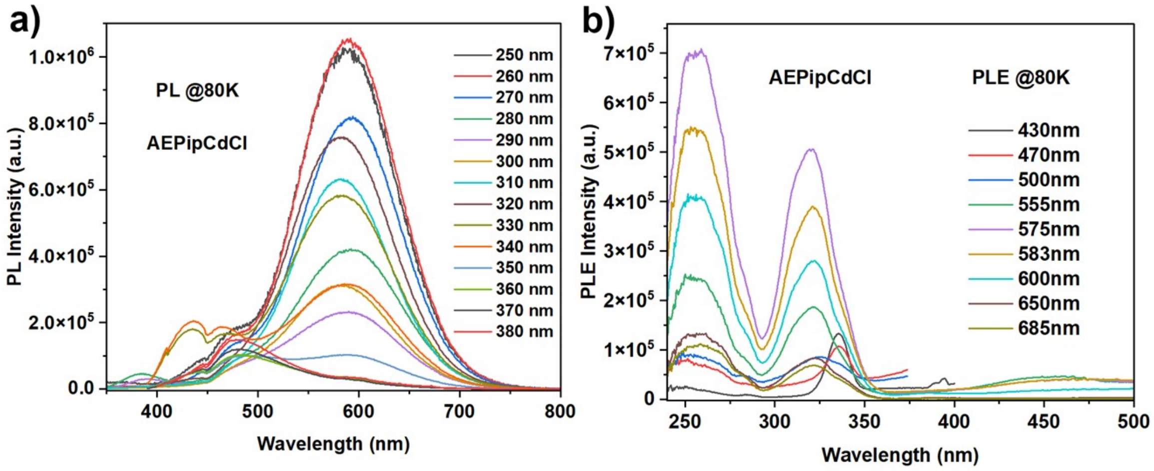

Figure S15: a) PL and b) PLE of AEPipCdCl collected at different excitation and emission wavelengths at 80 K respectively.

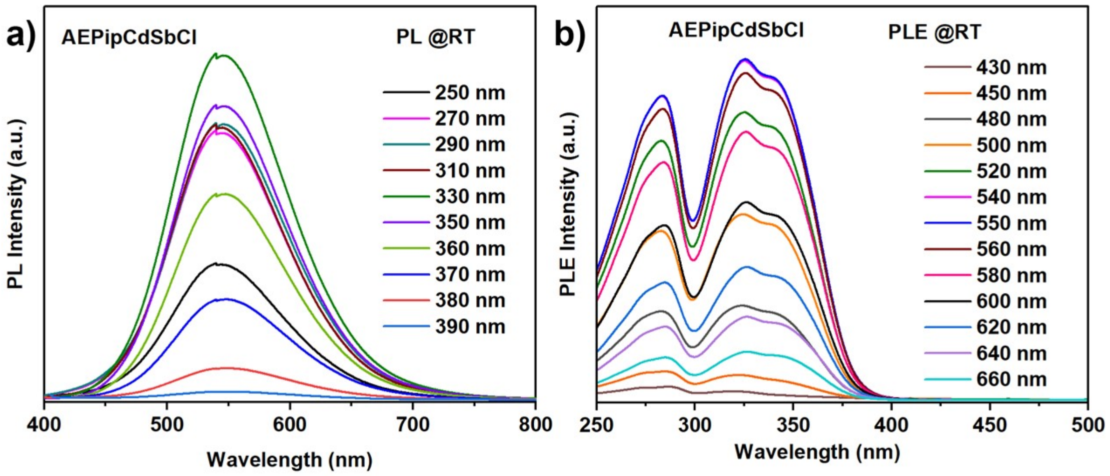

Figure S16: Room temperature a) PL and b) PLE of AEPipCdSbCl: Sb 5% system collected at different excitation and emission wavelengths.

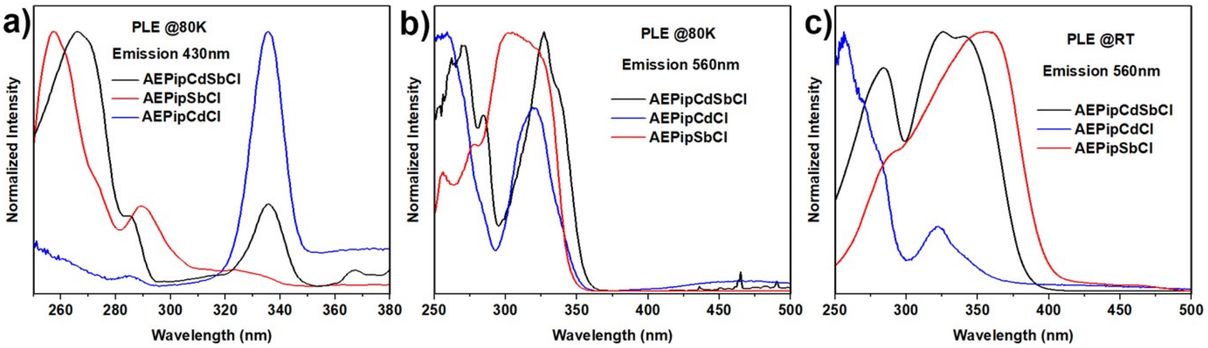

Figure S17: PLE comparison between AEPipCdSbCl: Sb 5%, AEPipCdCl, and AEPipSbCl at 80 K for a) 430 nm emission; b) 560 nm emission; and c) PLE comparison at room temperature for emission at 560 nm emission.

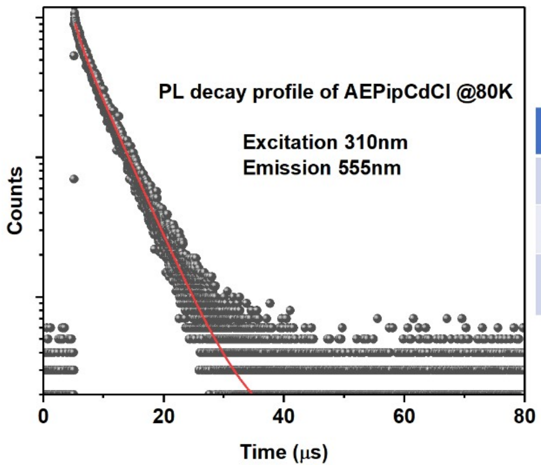

AEPipCdCl		
τ_1	4.68 μs	94.64%
τ_2	1.11 μs	5.36%
$\tau_{average}$ = 4.5 μs		

Figure S18: PL decay curve and corresponding lifetime value of host AEPipCdCl collected for 555 nm emission by exciting at 310 nm at 80 K.

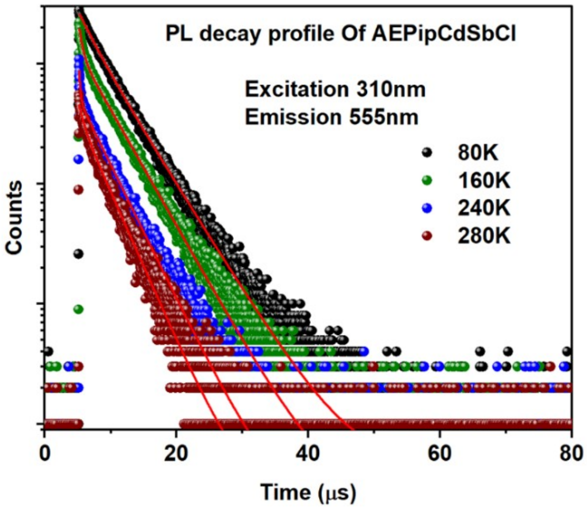

Figure S19: PL decay curve of AEPipCdSbCl: Sb 5% system at different temperatures.

Table S5: PL lifetime values of AEPipCdSbCl: Sb 5% system at different temperatures.

AEPipCdSbCl					
Temperature (K)	**τ_1(μs)**	**Rel%**	**τ_2 (μs)**	**Rel%**	**$\tau_{average}$ (μs)**
80K	**4.96 μs**	**85.27 %**	**2.43 μs**	**14.73 %**	**4.6 μs**
160K	**4.49 μs**	**92.89 %**	**0.51 μs**	**7.11 %**	**4.2 μs**
240K	**3.88 μs**	**95.96 %**	**0.19 μs**	**4.04 %**	**3.7 μs**
280K	**3.49 μs**	**93.26 %**	**0.73 μs**	**6.74 %**	**3.3 μs**

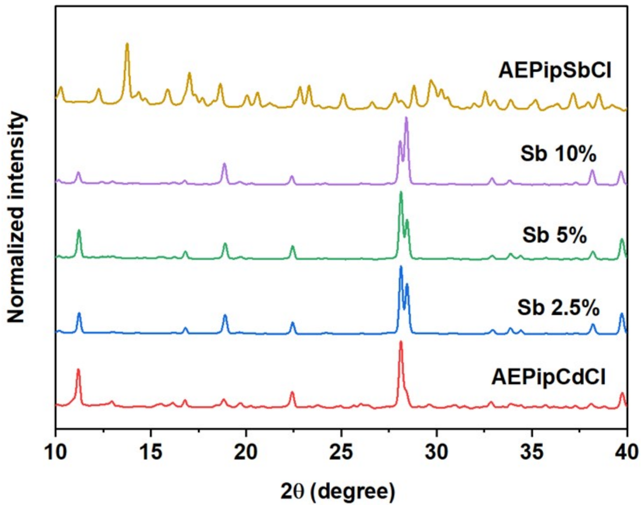

Figure S20: PXRD comparison of AEPipCdCl with different feed concentration (%) of Sb.

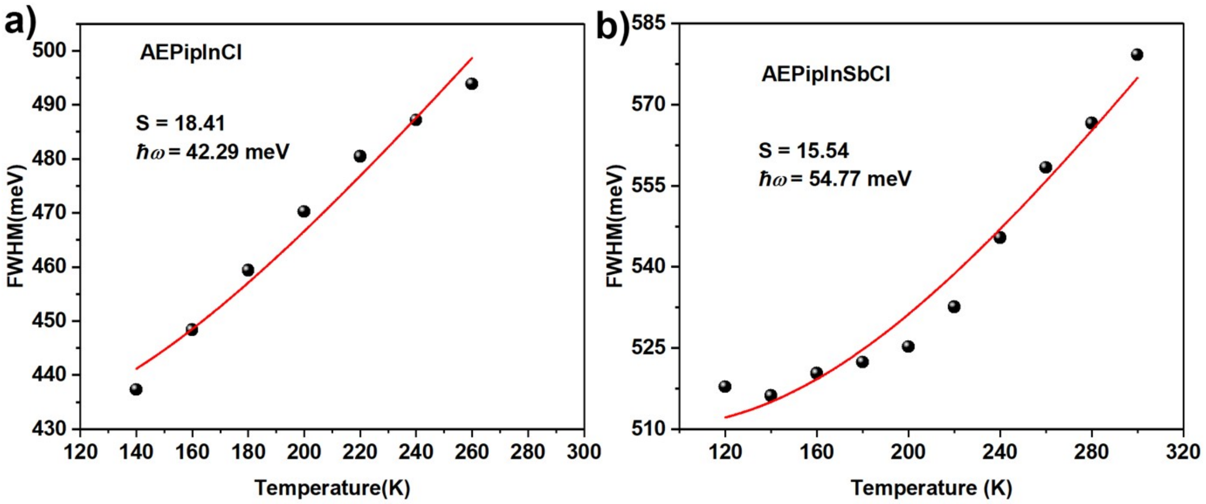

Figure S21: Fitted result of FWHM of PL peak with temperature and corresponding electron-phonon coupling parameter ‘*S*’, phonon frequency ‘ħω*’* for a) AEPipInCl, b) AEPipInSbCl: Sb 5% system respectively.

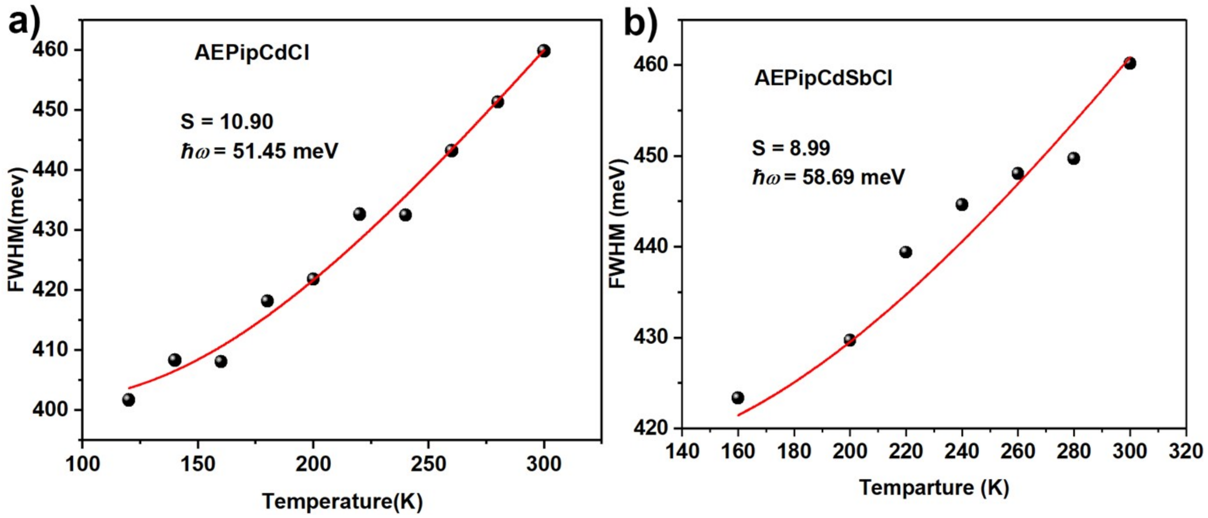

Figure S22: Fitted result of FWHM of PL peak with temperature and corresponding electron-phonon coupling parameter ‘*S*’, phonon frequency ‘ħω*’* for a) AEPipCdCl, b) AEPipCdSbCl: Sb 5% system respectively.

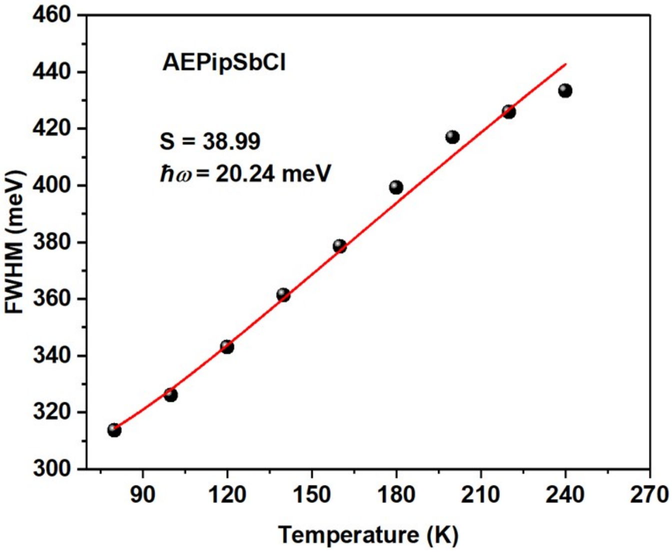

Figure S23: Fitted result of FWHM of PL peak with temperature and corresponding electron-phonon coupling parameter ‘*S*’, phonon frequency ‘ħω’ for AEPipSbCl system.

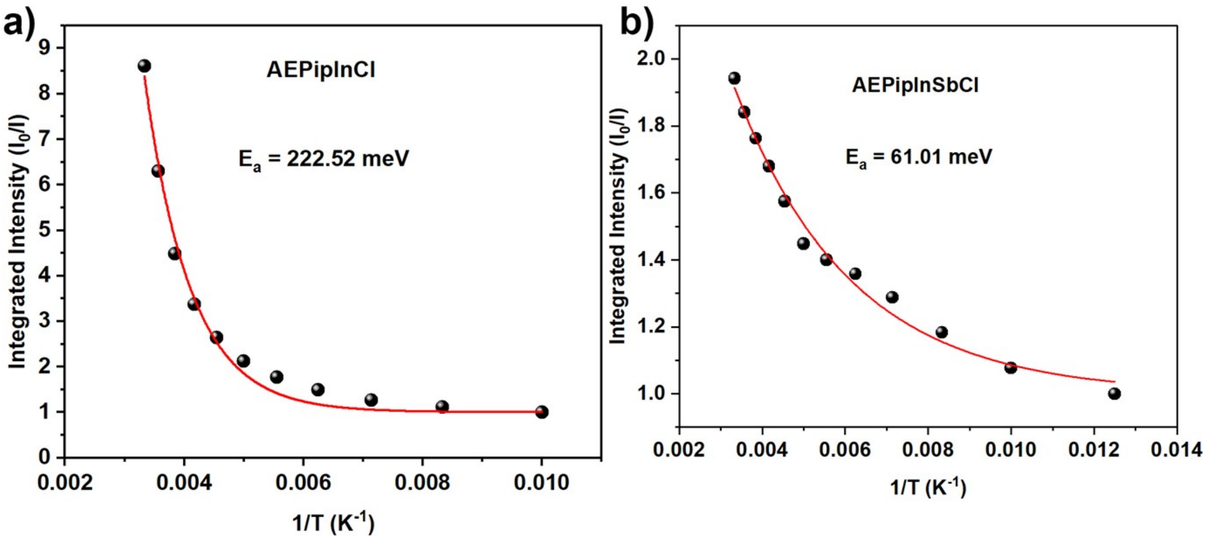

Figure S24: Fitted result of integrated intensity with temperature for a) AEPipInCl, b) AEPipInSbCl: Sb 5% system with estimated activation energy values (E_a).

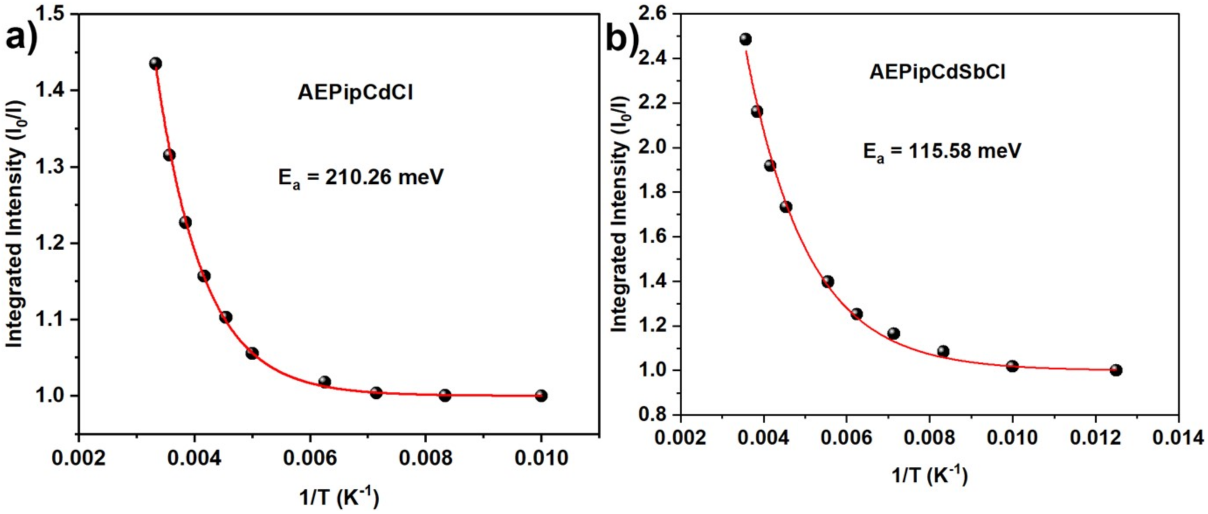

Figure S25: Fitted result of integrated intensity with temperature for a) AEPipCdCl, b) AEPipCdSbCl: Sb 5% system with estimated activation energy values (E_a).

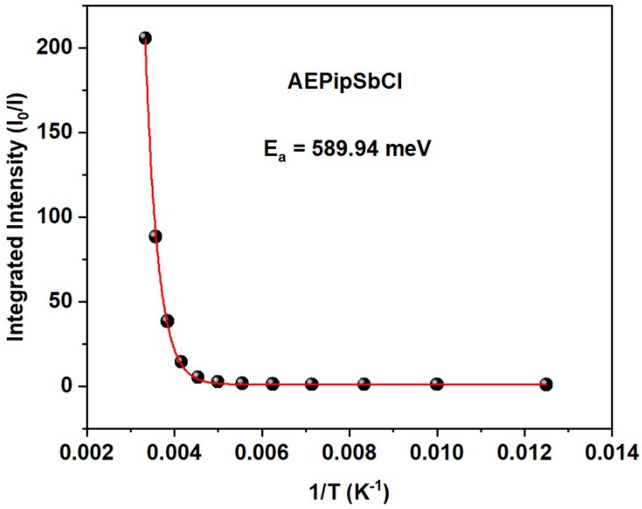

Figure S26: Fitted result of integrated intensity with temperature for AEPipSbCl with estimated activation energy value (E_a).

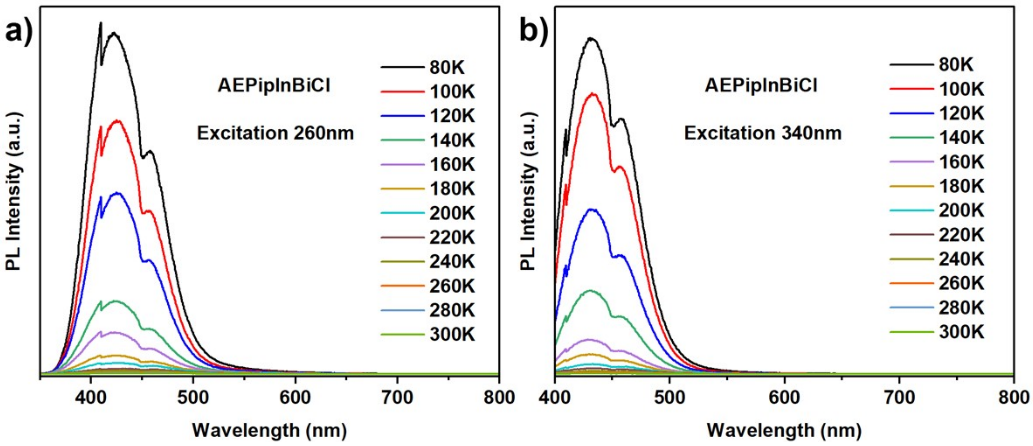

Figure S27: Temperature-dependent PL of AEPipInBiCl: Bi 10% system collected at a) 260 nm excitation; and b) 340 nm excitation respectively.

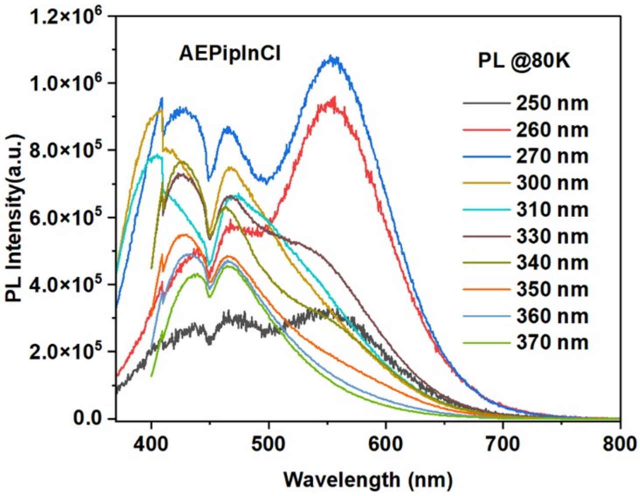

Figure S28: PL of AEPipInCl system collected at different excitation wavelengths at 80 K.

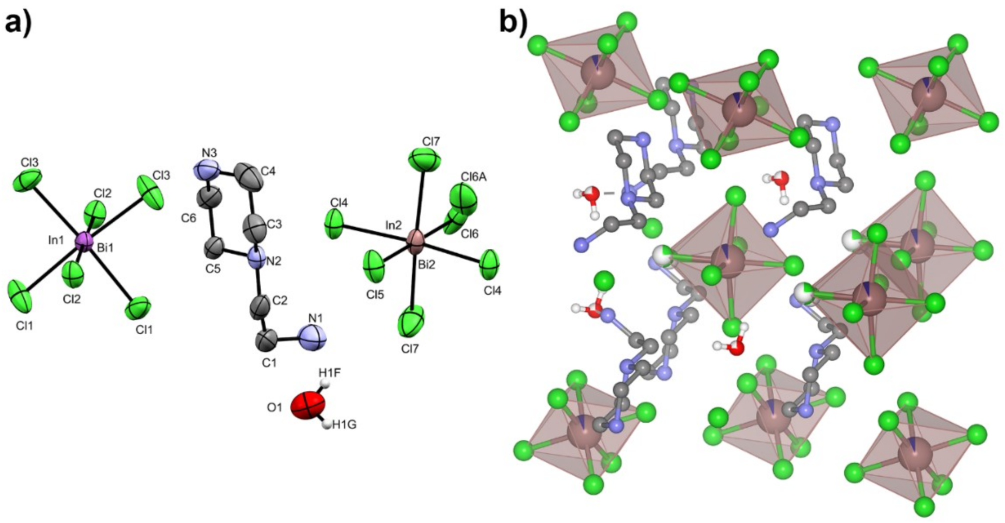

Figure S29: SCXRD structure of AEPipInBiCl: Bi 10% system showing a) the unit cell and b) packing diagram.

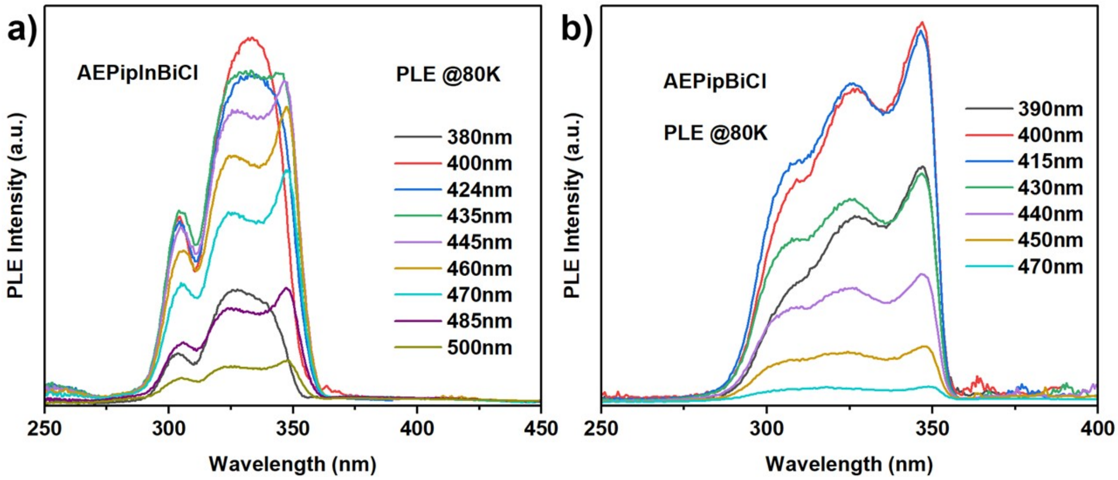

Figure S30: PLE at 80 K for a) AEPipInBiCl: Bi 10% system; b) AEPipBiCl collected at different emission wavelengths.

Table S6: Single Crystal data and structure refinement details.

Sample	AEPipInSbCl	AEPipCdCl	AEPipCdSbCl	AEPipInBiCl
Empirical formula	$C_{12}H_{40}Cl_{12}In_{1.4}N_6O_2Sb_{0.6}$	$C_{18}H_{61}Cd_2Cl_{14}N_9O_3$	$C_{18}H_{61}Cd_{1.88}Cl_{14}N_9O_3Sb_{0.12}$	$C_{12}H_{40}In_{1.86}Cl_{12}N_6O_2Bi_{0.14}$
Moiety formula	$(C_6H_{18}N_3)_2(In_{0.7}Sb_{0.3}Cl_6)_2.2(H_2O)$	$(C_6H_{18}N_3)_3(CdCl_6)_2.2Cl.2(H_2O).H_3O$	$(C_6H_{18}N_3)_3(Cd_{0.94}Sb_{0.06}Cl_6)_2.2Cl.2(H_2O).H_3O$	$(C_6H_{18}N_3)_2(In_{0.93}Bi_{0.07}Cl_6)_2.2(H_2O)$
Formula weight	479.85	1172.85	1173.98	484.24
Crystal system	orthorhombic	triclinic	triclinic	orthorhombic
Space group	$C222_1$	P-1	P-1	$C222_1$
a/Å	9.2822(3)	11.3496(5)	11.2977(4)	9.3694(3)
b/Å	12.7801(5)	12.0381(5)	11.9852(4)	12.8163(5)
c/Å	27.5406(10)	15.9352(6)	15.9247(6)	27.5560(10)
α/°	90	94.223(2)	93.9280(10)	90
β/°	90	95.077(2)	95.1080(10)	90
γ/°	90	90.437(2)	90.6180(10)	90
Volume/Å^3	3267.1(2)	2162.54(15)	2142.37(13)	3309.0(2)
Z	8	2	2	8
ρ_{calc}g/cm^3	1.951	1.801	1.820	1.944
μ/mm^{-1}	2.490	1.884	1.918	3.021
F(000)	1893.0	1180.0	1181.0	1907.0
Crystal size/mm^3	0.24 × 0.22 × 0.2	0.23 × 0.22 × 0.2	0.25 × 0.24 × 0.22	0.22 × 0.21 × 0.2
Radiation	MoKα (λ = 0.71073)	MoKα (λ = 0.71073)	MoKα (λ = 0.71073)	MoKα (λ = 0.71073)
2Θ range for data collection/°	5.424 to 53.998	3.604 to 51.996	3.62 to 53.99	5.386 to 52.812
Index ranges	$-11 \le h \le 11$, $-16 \le k \le 16$, $-35 \le l \le 35$	$-13 \le h \le 13$, $-14 \le k \le 14$, $-19 \le l \le 19$	$-14 \le h \le 14$, $-15 \le k \le 15$, $-20 \le l \le 20$	$-11 \le h \le 11$, $-16 \le k \le 16$, $-34 \le l \le 33$
Reflections collected	63467	104739	92965	25177
Independent reflections	3568 [R_{int} = 0.0569, R_{sigma} = 0.0189]	8447 [R_{int} = 0.0572, R_{sigma} = 0.0221]	9344 [R_{int} = 0.0347, R_{sigma} = 0.0221]	3393 [R_{int} = 0.0678, R_{sigma} = 0.0300]
Data/restraints/parameters	3568/0/161	8447/0/431	9344/6/446	3393/0/172
Goodness-of-fit on F^2	1.067	1.036	1.081	1.069
Final R indexes [I>=2σ (I)]	R_1 = 0.0271, wR_2 = 0.0706	R_1 = 0.0307, wR_2 = 0.0717	R_1 = 0.0232, wR_2 = 0.0544	R_1 = 0.0260, wR_2 = 0.0692
Final R	R_1 = 0.0275,	R_1 = 0.0344,	R_1 = 0.0245, wR_2 =	R_1 = 0.0302,

indexes [all data]	wR_2 = 0.0709	wR_2 = 0.0748	0.0551	wR_2 = 0.0700
Largest diff. peak/hole / e Å^{-3}	1.32/-0.92	2.02/-1.68	0.93/-0.93	1.12/-0.57
Flack parameter	0.28(3)	-	-	0.46(3)

Details of SCXRD data collection-

Single-crystal X-ray diffraction data were collected on a Bruker APEX II single-crystal X-ray CCD diffractometer having graphite monochromatized (Mo Kα, λ = 0.71073 Å) radiation at 100.0 K. Data reduction was performed using APEX II software.[1] Intensities for absorption were corrected with SADABS, and using Olex2 software[2], the structure was solved with the SHELXS[3] structure solution program using direct methods and refined with the SHELXL[4] refinement package using least-squares minimization, with anisotropic displacement parameters for all non-H atoms. In all crystal structures, hydrogen atoms were located through the Fourier difference electron density maps. Mercury software was used to prepare ORTEPs and packing diagrams.[5]

References:

1) Bruker. APEX2, SAINT, and SADABS; Bruker AXS Inc.: Madison, Wisconsin, 2012.

2) Dolomanov, O. V.; Bourhis, L. J.; Gildea, R. J.; Howard, J. A. K.; Puschmann, H. OLEX2: a complete structure solution, refinement and analysis program. J. Appl. Crystallogr. 2009, 42, 339−341.

3) Sheldrick, G. A short history of SHELX. Acta. Crystallogr. A. 2008, 64, 112−122.

4) Sheldrick, G. Crystal structure refinement with SHELXL. Acta. Crystallogr. C. 2015, 71, 3−8.

5) Macrae, C. F.; Edgington, P. R.; McCabe, P.; Pidcock, E.; Shields, G. P.; Taylor, R.; Towler, M.; van de Streek, J. Mercury: visualization and analysis of crystal structures. J. Appl. Crystallogr. 2006, 39, 453−457.